REVIEW OF COMPUTER ENGINEERING STUDIES

ISSN: 2369-0755 (Print), 2369-0763 (Online)
Vol.3, No. 1, March 2016, pp. 1-5
DOI: 10.18280/rces.030101

A publication of IIETA

International Information and Engineering Technology Association
Advancing the World of Information and Engineering
http://www. iieta. org/Journals/RCES

The Dynamic Phasor Model of Hybrid Micro Grid System

Hua Li * and Le Li

School of electric power college, Inner Mongolia University of Technology,
Hohhot, Aimin Street 49, 010051, China.

Email: lihua0806@qq.com

ABSTRACT

For hybrid micro grid system, this paper is established the dynamic phasor model based on the micro grid branch model and the system load line model of micro grid. In order to study micro power grid operation control and energy optimization problem, considering the accuracy and rapidity of the models, the micro power grid dynamic phasor model is put forward and set up including micro power supply and power electronic converter. The simulation analysis is carried out, and is validated the feasibility and superiority of the model. This model lay the foundation for the whole micro grid system optimization control and energy management research.

Keywords: Hybrid micro grid, Dynamic phasor model, Modeling and simulation.

1. INTRODUCTION

Because the hybrid micro grid system contains various types, a lot of power electronic converter, important and not important elements such as load and transmission lines, so to establish the system of mechanical and electrical or electromagnetic transient model model are difficult and simulation run slower.

In order to study the micro power grid operation control and energy optimization management, considering the accuracy of the models and the quickness of operation [1-6]. The dynamic phasor model is an effective modeling method of hybrid micro grid. Dynamic phasor model belongs to the dynamic model of a general average essentially, that is, the model can be modeled under certain conditions equivalent to time domain model [7-15]. The dynamic phasor model is based on Fourier series as the theoretical basis to establish its mathematical model.So far, the dynamic phasor model is used in motor control commonly, power system analysis and transmission, and application in the micro grid system is less.

2. THE DYNAMIC PHASOR MODEL OF CONVERTER

As shown in figure 1, it is given by the composition and includes converter of micro power grid structure, both through their respective branch and micro grid connected point of common coupling (PCC).Figure of each symbol in the content is as follows: u_{Li} is DG_i the voltage of the machine; R_i is the resistance of DG_i branch line; L_i is the inductance value of DG_i branch line; u_s is the PCC voltage. Below as well as its branch line, load and converter as an example, its corresponding dynamic phasor model is set up.

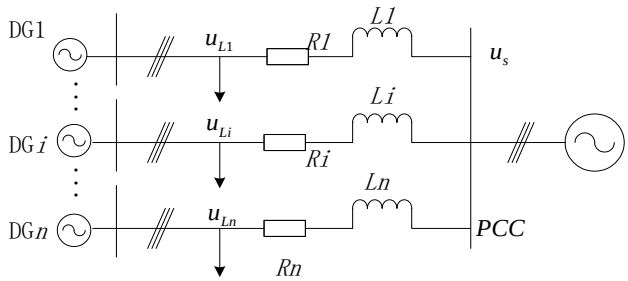

Figure 1. The diagrame of a microgrid

The DG1 branch topological structure of micro power grid is shown in figure 2, which adopts PQ control method, the specific structure of the controller is shown in figure 3 Graph. In the diagram, u_{abc}, i_{abc} is the voltage and current of machine side inverter respectively; $C_{abc/dq}$ is the constant power Park transformation, and its inverse transform is satisfy. $C_{dq/abc} = C_{abc/dq}^{-1} = C_{abc/dq}^{T}$.

$$C_{abc/dq} = \sqrt{\frac{2}{3}} \begin{bmatrix} \cos(\omega t) & \cos\left(\omega t - \frac{2\pi}{3}\right) & \cos\left(\omega t + \frac{2\pi}{3}\right) \\ -\sin(\omega t) & -\sin\left(\omega t - \frac{2\pi}{3}\right) & -\sin\left(\omega t + \frac{2\pi}{3}\right) \end{bmatrix} \quad (1)$$

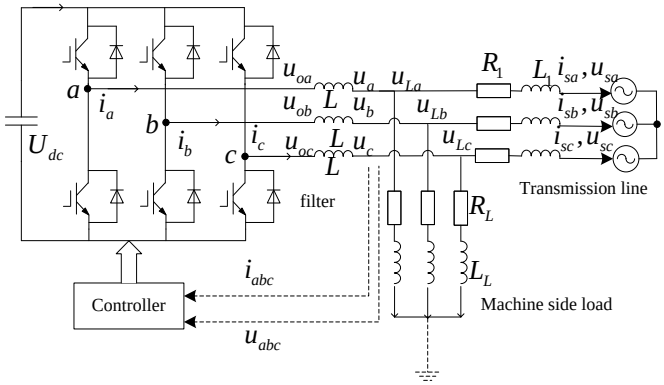

Figure 2 . The Circuit model of microgrid DG1 branch

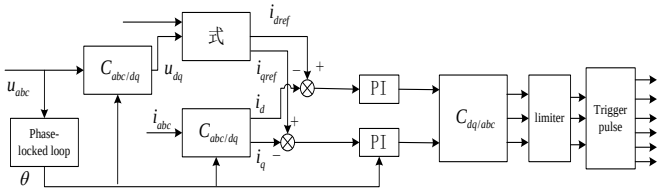

Figure 3. Configuration of the controller

By the output power of inverter instruction value P and Q be the dq axis current reference is:

$$\begin{cases} i_{dref} = \left(u_d P + u_q Q\right) / \left(u_d^2 + u_q^2\right) \\ i_{qref} = \left(u_q P - u_d Q\right) / \left(u_d^2 + u_q^2\right) \end{cases} \tag{2}$$

The instantaneous power relationship between power and current reference values as shown below:

$$\begin{cases} P = u_d i_{dref} + u_q i_{qref} \\ Q = u_d i_{dref} - u_q i_{qref} \end{cases} \tag{3}$$

By figure 3, the generation of pulse width modulation (PWM) trigger pulse is through the i_d, i_q of d, q axial by three phase current Park trans formation firstly. Then compared with the given reference current deviation, the deviation value through the PI regulator, that can obtain axial modulation signal. At last, the control circuit trigger pulse is obtained though comparing the modulation signal into inverse transform with triangular carrier.

The dynamic model of the three-phase symmetrical grid inverter is as follows:

$$L\dot{i} = u_o - u - Ri \tag{4}$$

Type: L is the filter inductance, $L = diag\left(L, L, L\right)$;

$R = diag\left(R, R, R\right)$ is the parasitic resistance between H bridge and the filter inductance and. Machine side current vector is $i = \left[i_a, i_b, i_c\right]^T$.

Inverter output voltage vector is $u_o = \left[u_{oa}, u_{ob}, u_{oc}\right]^T$. Machine terminal voltage vector is $u = \left[u_a, u_b, u_c\right]^T$ .In a phase for example, fundamental component dynamic phasor model is obtain as:

$$\begin{cases} Ld\left\langle i_a\right\rangle_1 / dt = -j\omega\left\langle i_a\right\rangle_1 + \left\langle u_{oa}\right\rangle_1 - \left\langle u_a\right\rangle_1 - R\left\langle i_a\right\rangle_1 \\ Ld\left\langle i_a\right\rangle_{-1} / dt = -j\omega\left\langle i_a\right\rangle_{-1} + \left\langle u_{oa}\right\rangle_{-1} - \left\langle u_a\right\rangle_{-1} - R\left\langle i_a\right\rangle_{-1} \end{cases} \tag{5}$$

In the type (5) $\omega = 2\pi f = 100\pi$. Because $\left\langle i_a\right\rangle_1 = \left\langle i_a\right\rangle_{-1}^*$ So, just consider one order dynamic phasor, which the real part and imaginary part of the amount for the dynamic equation is as follow:

$$\begin{cases} Ld\left\langle i_a\right\rangle_1^R / dt = \left\langle u_{oa}\right\rangle_1^R - \left\langle u_a\right\rangle_1^R - R\left\langle i_a\right\rangle_1^R + \omega L\left\langle i_a\right\rangle_1^I \\ Ld\left\langle i_a\right\rangle_1^I / dt = \left\langle u_{oa}\right\rangle_1^I - \left\langle u_a\right\rangle_1^I - R\left\langle i_a\right\rangle_1^I - \omega L\left\langle i_a\right\rangle_1^R \end{cases} \tag{6}$$

B and C phase dynamic phasor equation is available in the same way as:

$$\begin{cases} Ld\left\langle i_b\right\rangle_1^R / dt = \left\langle u_{ob}\right\rangle_1^R - \left\langle u_b\right\rangle_1^R - R\left\langle i_b\right\rangle_1^R + \omega L\left\langle i_b\right\rangle_1^I \\ Ld\left\langle i_b\right\rangle_1^I / dt = \left\langle u_{ob}\right\rangle_1^I - \left\langle u_b\right\rangle_1^I - R\left\langle i_b\right\rangle_1^I - \omega L\left\langle i_b\right\rangle_1^R \\ Ld\left\langle i_c\right\rangle_1^R / dt = \left\langle u_{oc}\right\rangle_1^R - \left\langle u_c\right\rangle_1^R - R\left\langle i_c\right\rangle_1^R + \omega L\left\langle i_c\right\rangle_1^I \\ Ld\left\langle i_c\right\rangle_1^I / dt = \left\langle u_{oc}\right\rangle_1^I - \left\langle u_c\right\rangle_1^I - R\left\langle i_c\right\rangle_1^I - \omega L\left\langle i_c\right\rangle_1^R \end{cases} \tag{7}$$

If the machine side voltage of positive sequence fundamental component is as follows:

$$\begin{cases} u_a = E\sin\left(\omega t + \phi\right) \\ u_b = E\sin\left(\omega t - 2\pi/3 + \phi\right) \\ u_c = E\sin\left(\omega t + 2\pi/3 + \phi\right) \end{cases} \tag{8}$$

On the type of each in conformity with the said content is as follows: E is the amplitude of the input voltage of the machine; ϕ is the phase voltage of the machine.

By type (7) and (8) obtained:

$$\begin{cases} \left\langle u_a\right\rangle_1 = Ee^{j(\phi - \pi/2)} / 2 \\ \left\langle u_b\right\rangle_1 = Ee^{j(\phi - 2\pi/3 - \pi/2)} / 2 \\ \left\langle u_c\right\rangle_1 = Ee^{j(\phi + 2\pi/3 - \pi/2)} / 2 \end{cases} \tag{9}$$

Will type (9) combine with the 1 order dynamic phase value of control signal, which can known 1 order dynamic phasor relationship of grid inverter output voltage is as follows:

$$\begin{bmatrix} \left\langle u_a\right\rangle_1 \\ \left\langle u_b\right\rangle_1 \\ \left\langle u_c\right\rangle_1 \end{bmatrix} = K_{pwm} C_{dq/abc} \begin{bmatrix} \left\langle u_d\right\rangle_1 \\ \left\langle u_q\right\rangle_1 \end{bmatrix} \tag{10}$$

On the type: K_{pwm} is the equivalent ratio of grid inverter, for the three-phase bridge inverter, available:

$K_{pwm}=U_{dc}/2$; $\langle u_d\rangle_1$, $\langle u_q\rangle_1$ is the PI dq axial current regulator output signal, then:

$$\begin{cases}\langle u_d\rangle_1=\left(K_P+K_i/s\right)\left(i_{dref}-\langle i_d\rangle_1\right)\\ \langle u_q\rangle_1=\left(K_P+K_i/s\right)\left(i_{qref}-\langle i_q\rangle_1\right)\end{cases} \tag{11}$$

In a phase for example, available:

$$\begin{aligned}&\langle u_{oa}\rangle_1=\sqrt{2/3}K_{pwm}\left[\langle u_d\rangle_1\cos(\omega t)-\langle u_q\rangle_1\sin(\omega t)\right]=\\ &\sqrt{2/3}K_{pwm}\sqrt{\langle u_d\rangle_1^2+\langle u_q\rangle_1^2}\cos(\omega t+\phi)=\\ &K_{pwm}\sqrt{\frac{1}{6}}\sqrt{\langle u_d\rangle_1^2+\langle u_q\rangle_1^2}e^{j\phi}\end{aligned} \tag{12}$$

The phase Angle in type is $\phi=\arctan\left(\langle u_q\rangle_1/\langle u_d\rangle_1\right)$.
Similarly for b and c phase as:

$$\begin{cases}\langle u_{ob}\rangle_1=K_{pwm}\sqrt{\frac{1}{6}}\sqrt{\langle u_d\rangle_1^2+\langle u_q\rangle_1^2}e^{j(\phi-2\pi/3)}\\ \langle u_{oc}\rangle_1=K_{pwm}\sqrt{\frac{1}{6}}\sqrt{\langle u_d\rangle_1^2+\langle u_q\rangle_1^2}e^{j(\phi+2\pi/3)}\end{cases} \tag{13}$$

3. THE DYNAMIC PHASOR MODEL OF MICRO GRID SYSTEM LOAD AND LINE

Figure 4(a) shows the dynamic equation of transmission line is as follows:

$$\Delta u=L_1\frac{di}{dt}+R_1 i \tag{14}$$

By the definition of the dynamic phasor model, dynamic phasor of the transmission line is as follows:

$$\langle\Delta u\rangle_1=L_1\frac{d\langle i\rangle_1}{dt}+j\omega L_1\langle i\rangle_1+R_1\langle i\rangle_1 \tag{15}$$

In figure 4(b) as shown in the sense of resistance load are:

$$\begin{cases}L_L d\langle i_{LR}\rangle_1^R/dt=\langle u_L\rangle_1^R+\omega L_L\langle i_{LR}\rangle_1^I-R_L\langle i_{LR}\rangle_1^R\\ L_L d\langle i_{LR}\rangle_1^I/dt=\langle u_L\rangle_1^I-\omega L_L\langle i_{LR}\rangle_1^R-R_L\langle i_{LR}\rangle_1^I\end{cases} \tag{16}$$

Same as above principle, in the type (16), the impedance load dynamic phasor model is obtained via making the $L_L=0$ in figure 4(c). The perceptual load dynamic phasor model is shown via making the $R_L=0$.

In the same way, the DG2, DG3 branch dynamic phasor model can also be set up like the above DG1 branch dynamic phasor model, and no give unnecessary details here.

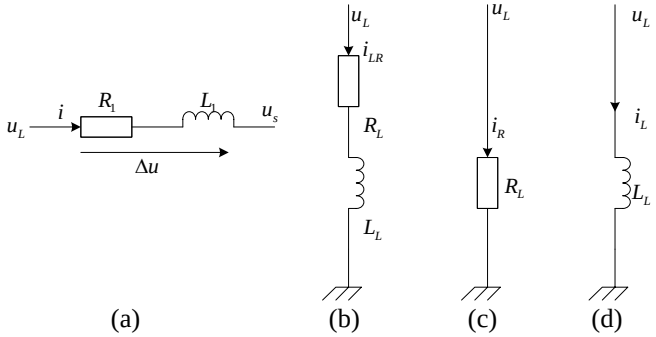

Figure 4. The dynamic phasors modeling of microgrid loads and transmission line

4. THE SIMULATION STRUCTURE AND ANALYSIS

4.1 The simulation parameters

In an effort figure 5 micro power grid structure is as an example, the micro grid system is composed of three DG branch, each DG connected to the PCC point of transmission line length is not equal, including specific length as shown in table 1.

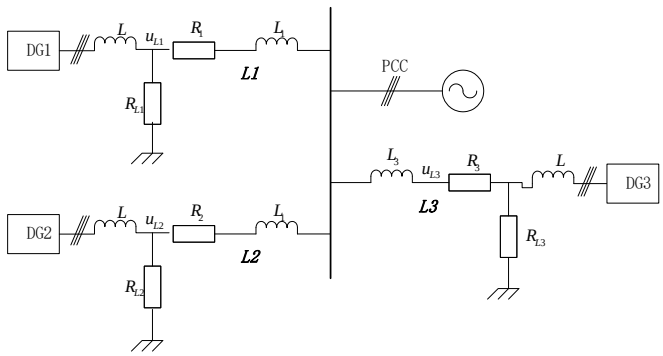

Figure 5. Verify the dynamic model of micro power grid structure

Table 1. System parameters

The parameter types	The numerical size
Per kilometre of line resistance	$0.642\left(\Omega/km\right)$
Per kilometre of the line reactance	$0.083\left(\Omega/km\right)$
DG Switching frequency	8 (f_s/KHz)
DC bus voltage of DG	700 (U_{dc}/V)
DG filtering inductance	2 (L/mH)
The parasitic resistance between H bridge and filter inductance in DG	$0.1/\Omega$
The DG proportion of current control loop parameters K_P	10
DG Current control loop integral parameter K_i	1000

Table 1 shows the low line belongs to the impedance parameters, impedance ratio of 7.7:1, PCC is the low voltage power distribution network, the RMS voltage is 220 v. The length of the line L1, L2 and L3 is 0.3 km, 0.4 km and 0.2 km separately. All the sets of DG connects with the three-phase symmetrical machine load, DG1, DG2 resistance load size is $R_{L1}=30\Omega, R_{L2}=50\Omega$, the size of the DG3 every phase load values is $R_{L3}=40\Omega, L_{L3}=50mH$.

4.2 The simulation results

The hybrid micro grid dynamic phasor model is established as shown in figure 6 based on the grid inverter, transmission line and load dynamic phasor model. And DG1 simulation model structure is shown in figure 7. The simulation model of DG2 and DG3 is like DG1, that is needless is here.

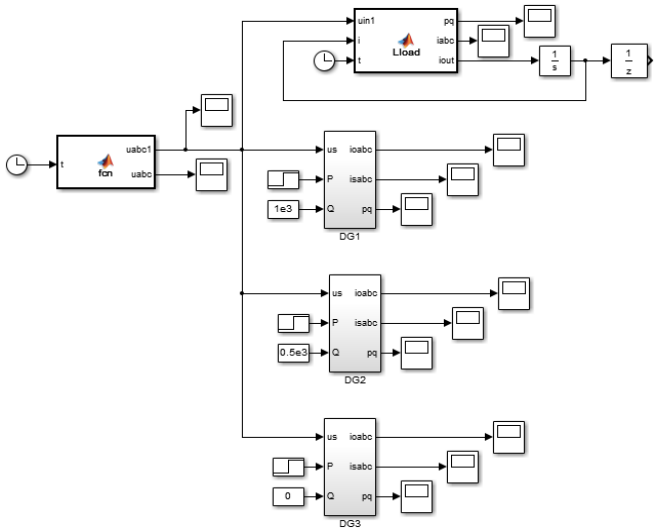

Figure 6. The micro grid Matlab/Simulink dynamic phasor model

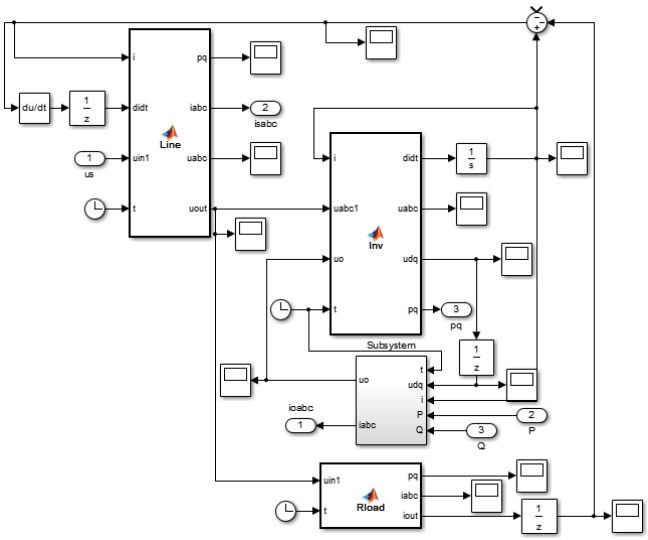

Figure 7. DG1 internal simulation model

When hybrid micro grid system operated at 0.1s, making the DG1 active power break from 3Kw to 5Kw, DG2 active power instructions break from 2Kw to 3.5Kw, DG3 active power instruction break from 1Kw to 2.5Kw.The reactive power of the DG order value 1 kvar, respectively, 0.5 kvar with 0 kvar.

Figure 8 shows the DG of the instantaneous active and reactive power dynamic phasor model results. Figure 9 shows the DG each of type a, b, c camera dynamic phasor current waveform structure.

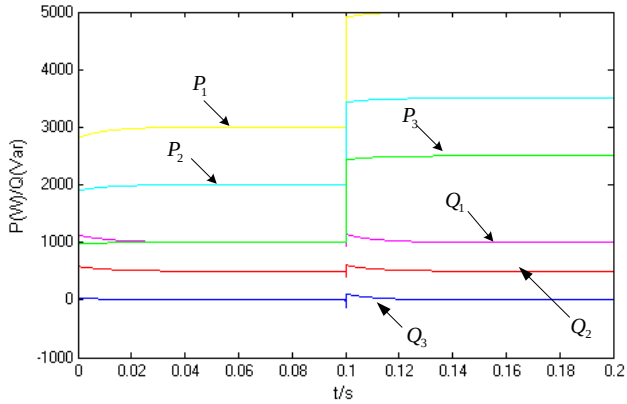

Figure 8. The power output diagram of DG1, DG2, DG3 active and reactive

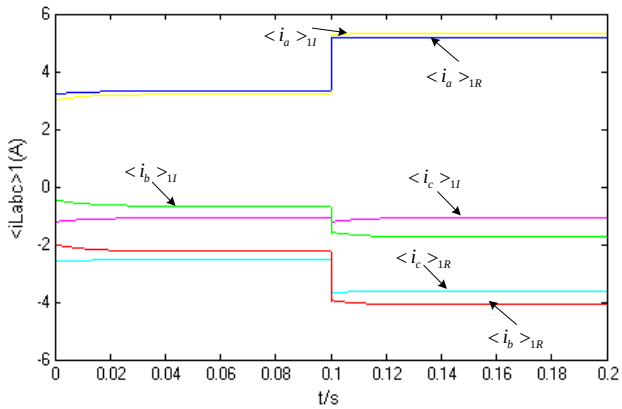

Figure 9. DG dynamic phasor current waveform

5. CONCLUSIONS

This paper establishes the micro grid dynamic phasor model including power electronics converter and different kinds of DG. Then the simulation model is built and verified under the Matlab/Simulink. The results show that: (1) the dynamic phasor model can reflect the dynamic characteristic of the hybrid micro grid containing the electronic converter preferably; (2) the dynamic phasor model computing speed of hybrid micro grid is fast.

REFERENCES

[1] Binayak Bhandari, Shiva Raj PoudeShiva Raj Poudel, Kyung-Tae Lee, et al., "Mathematical modeling of hybrid renewable energy system: A review on small hydro-solar-wind power generation," *International Journal of Precision Engineering and Manufacturing-Green Technology*, vol. 1, no. 2, pp. 157-173, 2014. DOI: 10.1007/s40684-014-0021-4.

[2] Binayak Bhandari, Kyung-Tae Lee, Gil-Yong Lee, et al., "Optimization of hybrid renewable energy power systems: A review," *International Journal of Precision Engineering and Manufacturing-Green Technology, vol. 2, no. 1*, pp. 1-14, 2015. DOI: 10.1007/s40684-015-0013-z.

[3] Camblong Haritza, Curea Octavian, Etxeberria Aitor, et al., "Research experimental platforms to study microgrids issues," *Int J Interact Des Manuf*, vol. 31, pp. 1-13, 2015. DOI: 10.1007/s12008-015-0288-x.

[4] Sohrab Mirsaeidi, Dalila Mat Said, Mohammad Wazir Mustafa, et al. "Design and testing of a centralized protection scheme for micro-grids," *J. Cent. South Univ.,* vol. 22, pp. 3876-3887, 2015. DOI: 10.1007/s11771-015-2932-9.

[5] Zina Boussaada, Octavian Curea, Haritza Camblong, et al. "Multi-agent systems for the dependability and safety of microgrids," *Int J Interact Des Manuf Int J Interact Des Manuf.,* vol. 30, pp. 1-13, 2014. DOI: 10.1007/s12008-014-0257-9.

[6] Ritwik Majumder, "A hybrid microgrid with DC connection at back to back converters," *IEEE TRANSACTIONS ON SMART GRID,* vol. 5, no. 1, pp. 251-259, 2014.

[7] Gabriella Ferruzzi, Giorgio Graditi, Federico Rossi, et al., "Optimal operation of a residential microgrid: The role of demand side management," *Intell Ind Syst,* vol. 1, pp. 61 – 82, 2015. DOI: 10.1007/s40903-015-0012-y.

[8] Babak Mozafari and Sirus Mohammadi, "Optimal sizing of energy storage system for microgrids," *Indian Academy of Sciences*, vol. 39, no. 4, pp. 819-841, 2014.

[9] V. Pavan Kumar and Ravikumar Bhimasingu, "Renewable energy based microgrid system sizing and energy management for green buildings," *J. Mod. Power Syst. Clean Energy,* vol. 3, no. 1, pp. 1-13, 2015. DOI: 10.1007/s40565-015-0101-7.

[10] Thongchart Kerdphol, Yaser Qudaih, Masayuki Watanabe, et al., "RBF neural network-based online intelligent management of a battery energy storage system for stand-alone microgrids," *Kerdphol et al. Energy, Sustainability and Society, vol. 6, no. 5*, pp. 1-16, 2016. DOI: 10.1186/s13705-016-0071-2.

[11] Sherali Zeadally, Al-Sakib Khan Pathan, Cristina Alcaraz, et al. "Towards privacy protection in smart grid," *Wireless Pers Commun*, vol. 73, pp. 23-50, 2013. DOI: 10.1007/s11277-012-0939-1.

[12] Yunwei Li and Farzam Nejabatkhah. "Overview of control, integration and energy management of microgrids," *J. Mod. Power Syst. Clean Energy,* vol. 2, no. 3, pp. 212-222, 2014. DOI: 10.1007/s40565-014-0063-1.

[13] Reza Roofegari Nejad and Seyed Masoud Moghaddas Tafreshi. "Operation planning of a smart microgrid including controllable loads and intermittent energy resources by considering uncertainties," *Arab J Sci Eng,* vol. 39, pp. 1-19, 2014. DOI: 10.1007/s13369-014-1267-4.

[14] Kubilay Demir, Daniel Germanus and Neeraj Suri. "Robust QoS-aware communication in the smart distribution grid," *Peer-to-Peer Netw. Appl..* vol. 24, pp. 1-15, 2015. DOI: 10.1007/s12083-015-0418-z.

[15] An Luo, Qianming Xu, Fujun Ma, et al., "Overview of power quality analysis and control technology for the smart grid," *J. Mod. Power Syst. Clean Energy,* vol. 4, no. 1, pp. 1-9, 2016. DOI: 10.1007/s40565-016-0185-8.